Supplemental Information

Extrasynaptic glutamate release through cystine/glutamate antiporter contributes to ischemic damage

Federico N. Soria, Alberto Pérez-Samartín, Abraham Martin, Kiran Babu Gona, Jordi Llop, Boguslaw Szczupak, Juan Carlos Chara, Carlos Matute and María Domercq.

(Supplemental information includes three figures, supplemental methods and supplemental references).

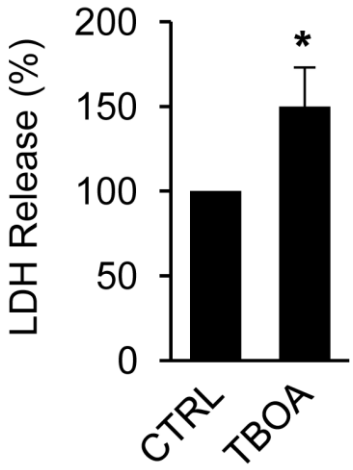

Supplemental Figure 1. Inhibition of glutamate transporters with TBOA is toxic to organotypic cortical cultures. Histogram shows LDH release in the absence or in the presence of EAATs inhibitor TBOA (100 μM, 24h, $n = 3$). These data are consistent with the idea that TBOA in normoxia is toxic to pyramidal neurons, as previously described (1–3). Data Data are expressed as mean ± SEM. *$p < 0.05$.

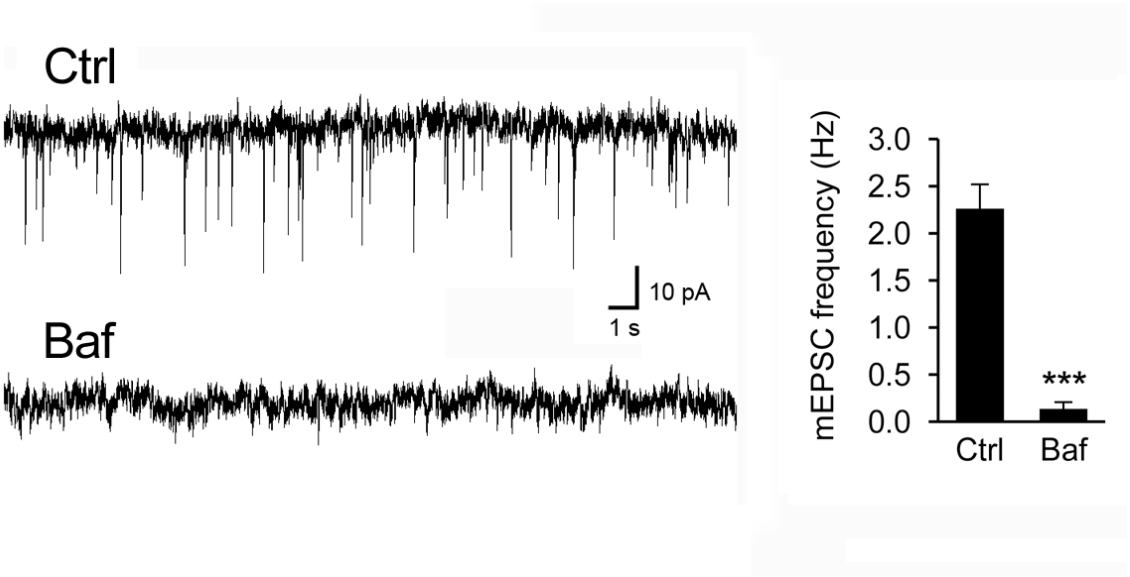

Supplemental Figure 2. Bafilomycin A1 effectively inhibits vesicular glutamate release**.** Electrophysiological recordings of mEPSCs in acute slices in the presence or absence of bafilomycin A1 (Baf, 1 μM) in rat cortical slices. Data are expressed as mean ± SEM (n= 3). ***$p < 0.001$.

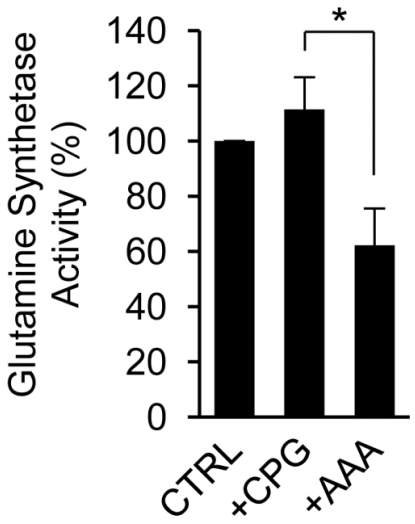

Supplemental Figure 3. Non-transportable system xc- inhibitor CPG (250 µM) does not interfere with glutamine synthetase (GS) activity. On the contrary, aminoadipic acid (AAA; 250 µM), a transportable inhibitor of cystine/glutamate antiporter and known inhibitor of GS, inhibits GS activity in cultured neurons. GS activity was measured on neuronal cultures using a previously described methodology (4) with minor modifications (See Supplementary Methods). Data are expressed as mean ± SEM. *$p < 0.05$

Supplemental Methods

mEPSCs recordings

Bafilomycin A1 was purchased from Tocris and was bath applied for ≥2 h (final concentration, 1 μM). Slices in the control group were simultaneously incubated in regular ACSF (without Bafilomycin A1) for the same amount of time. Miniature excitatory postsynaptic currents (mEPSCs) were recorded in pyramidal cortical neurons in acute slices in the presence of tetrodotoxin (TTX, 1 μM). A brief application (5s) of a high sucrose solution (adding 200 mM sucrose to the external solution) was applied to increase vesicle turnover.

In vitro ischemia

Chemical ischemia (1 h) in primary cortical neurons was achieved by replacing O_2 with N_2 and external glucose (10 mM) with sucrose (10 mM), and adding iodoacetate (50 μM) to block glycolysis in an extracellular solution containing 130 mM NaCl, 5.4 mM KCl, 1.8 mM $CaCl_2$, 26 mM $NaHCO_3$, 0.8 mM $MgCl_2$, and 1.18 mM NaH_2PO_4 (pH 7.4). After 1 h OGD, extracellular solution was replaced with medium and O_2 supply restored. Cell death was determined 24 h later using calcein-AM (Life Technologies) in a Synergy-HT fluorimeter (BioTek Instruments) as previously described (5).

Quantitative real-time PCR, Western blotting and ^{14}C-cystine uptake

Total RNA was isolated from primary cortical neuron cultures using TRIzol reagent (Life Technologies) according to the manufacturer's instructions. Subsequently, cDNA synthesis was conducted using SuperScript III retrotranscriptase (200 U/μl; Life Technologies) and random hexamers as primers. Primers for xCT and endogenous

genes and PCR conditions are described elsewhere (6). Total protein was obtained by scraping the cells in SDS/sample buffer. xCT expression was analyzed by conventional Western blot (6) using primary antibodies against xCT (0.25 μg/mL; AB37815, AbCam) and β-actin (1:5000; Sigma). The band analyzed for xCT expression was the 40 kDa band, which is the MW of the rat/mouse xCT band (7, 8), which has been found to be regulated by oxidative stress (9). The activity of cystine/glutamate antiporter was defined as the Cl^--dependent [^{14}C] L-cystine uptake. For that purpose, two different buffers were used: a complete buffer (pH 7.4) containing 140 mM NaCl, 5 mM KCl, 2 mM $MgCl_2$, 2 mM $CaCl_2$, 10 mM HEPES, and 25 mM glucose; and a Cl^--free buffer in which chloride was equimolarly replaced with gluconate. A time-course curve was constructed to determine time conditions when cystine uptake increased linearly, avoiding saturation of the transport systems. Briefly, control and OGD-exposed cells were rinsed three times in warmed buffer and then incubated for 5 min in the corresponding buffer containing [^{14}C] L-cystine (0.2 μCi/mL, 350 nM) plus cold L-cystine (10 μM). Uptake was finished by rinsing cells three times in ice-cold buffer, and cells were solubilized in 250 μl lysis solution (2.5 N NaOH, 0.01% Triton X-100 in 0.1 M PBS) and mixed with 2.5 mL scintillation liquid. Counts per minute were determined 24 h later in a liquid scintillation counter (Beckman Coulter).

Glutamine synthetase activity assay

The assay is based in previously described procedures (4) with minor modifications. Briefly, rat brains were homogenized in 0.1 M sodium acetate, pH 7.4 (10 μL/mg tissue), centrifuged at 1200 *g* (15 min) and the supernatant used for the assay. Activity of GS was measured according to the method described by Wellner and Meister (10), where hydroxylamine (200 mM) reacts with glutamine (100 mM) in presence of ATP (1

mM) and $MnCl_2$ (33 mM) to produce y-glutamylmono-hydroxymate, which subsequently reacts with $FeCl_3$ (0,37 M, dissolved in HCl 0,67 M) yielding a colorimetric product. The relatives quantities of y-glutamylmono-hydroxymate formed at 37ºC over 20 min were determined spectrophotometrically at 490 nm.

Radiochemistry

Synthesis of (4S)-4-[3-[^{18}F]fluoropropyl]-L-glutamate (FSPG) was performed by ^{18}F-fluorination of the protected precursor Di-tert-butyl-(2S,4S)-2-tert-butoxycarbonylamino-4-(3-nitrophenylsulfonyloxy-propyl)-pentanedioate followed by acidic hydrolysis, as previously described (11). For the labeling step, a method reported previously was followed (11) with minor modifications. Radiochemical yields (EOB) were in the range 30-35% and radiochemical purity was always >93% at the time of injection.

Positron Emission Tomography scans, data acquisition and image analysis

PET scans were performed in the ischemic rats (*n*=10) at 5 minutes and 5 hours after reperfusion as well as in non-operated rats used as controls (*n*=5) using a General Electric eXplore Vista CT camera. Scans were performed in rats anaesthetized with 4% isofluorane and maintained by 2-2.5% of isofluorane in 100% O_2. Around 40 MBq of [^{18}F]FSPG were injected intravenously via the tail vein concomitantly with the start of the PET acquisition. Brain dynamic images were acquired (34 frames: 6x5, 6x15, 6x60, 8x120, 8x300 seconds) in the 400-700 keV energetic window, with a total acquisition time of 64 minutes, providing 0.387 mm thick 175 transaxial and 0.775 mm thick 61 axial slices. After each PET scan, CT acquisitions were also performed (140 µA intensity, 40 kV voltage), providing anatomical information of each animal as well as

the attenuation map for the later image reconstruction. Dynamic acquisitions were reconstructed (decay and CT-based attenuation corrected) with filtered back projection (FBP) using a Ramp filter with a cutoff frequency of 1 Hz.

PET images were analyzed using PMOD image analysis software (PMOD Technologies). Two types of regions of interest (ROIs) were established to quantify the entire series of PET images: (i) A first set of ROIs was defined to study the ^{18}[F]FSPG uptake in the entire region affected by the ischemic lesion and in the contralateral hemisphere. These ROIs were manually defined on the territory irrigated by the middle cerebral artery of the ipsilateral hemisphere, as well as in the homologous contralateral hemisphere by using an MRI (T2W) rat template. (ii) A second set of VOIs were automatically generated in cortex and striatum by using the regions proposed by the PMOD rat brain template. For quantification, frames 30–34 (last 15 min of PET acquisition) were averaged and the uptake in each ROI (mean ± SD) was determined and expressed as percentage of injected dose per body weight (%ID/g) for both ischemic (ipsilateral) and the homologous contralateral regions. Results were considered as the ipsi-to-contralateral ratio of striatum, cortex and brain hemisphere PET signals.

Supplemental References

1. O'Shea RD, et al. Evaluation of drugs acting at glutamate transporters in organotypic hippocampal cultures: new evidence on substrates and blockers in excitotoxicity. *Neurochem Res*. 2002;27(1-2):5–13.

2. Bonde C, et al. GDNF pre-treatment aggravates neuronal cell loss in oxygen–glucose deprived hippocampal slice cultures: a possible effect of glutamate transporter up-regulation. *Neurochem Int*. 2003;43(4-5):381–388.

3. Colleoni S, et al. Neuroprotective effects of the novel glutamate transporter inhibitor (-)-3-hydroxy-4,5,6,6a-tetrahydro-3aH-pyrrolo[3,4-d]-isoxazole-4-carboxylic acid, which preferentially inhibits reverse transport (glutamate release) compared with glutamate reuptake. *J Pharmacol Exp Ther*. 2008;326(2):646–656.

4. McBean GJ. Inhibition of the glutamate transporter and glial enzymes in rat striatum by the gliotoxin, alpha aminoadipate. *Br J Pharmacol*. 1994;113(2):536–540.

5. Domercq M, et al. P2X7 receptors mediate ischemic damage to oligodendrocytes. *Glia*. 2010;58(6):730–740.

6. Pampliega O, et al. Increased expression of cystine/glutamate antiporter in multiple sclerosis. *J Neuroinflammation*. 2011;8(1):63.

7. Burdo J, Dargusch R, Schubert D. Distribution of the cystine/glutamate antiporter system xc- in the brain, kidney, and duodenum. *J Histochem Cytochem*. 2006;54(5):549–557.

8. La Bella V, Valentino F, Piccoli T, Piccoli F. Expression and developmental regulation of the cystine/glutamate exchanger (xc-) in the rat. *Neurochem Res*. 2007;32(6):1081–1090.

9. Mysona B, Dun Y, Duplantier J, Ganapathy V, Smith SB. Effects of hyperglycemia and oxidative stress on the glutamate transporters GLAST and system xc- in mouse retinal Müller glial cells. *Cell Tissue Res*. 2009;335(3):477–488.

10. Wellner VP, Zoukis M, Meister A. Acitivity of glutamine synthetase toward the optical isomers of alpha-aminoadipic acid. *Biochemistry*. 1966;5(11):3509–3514.

11. Koglin N, et al. Specific PET imaging of xC- transporter activity using a ^{18}F-labeled glutamate derivative reveals a dominant pathway in tumor metabolism. *Clin Cancer Res*. 2011;17(18):6000–6011.

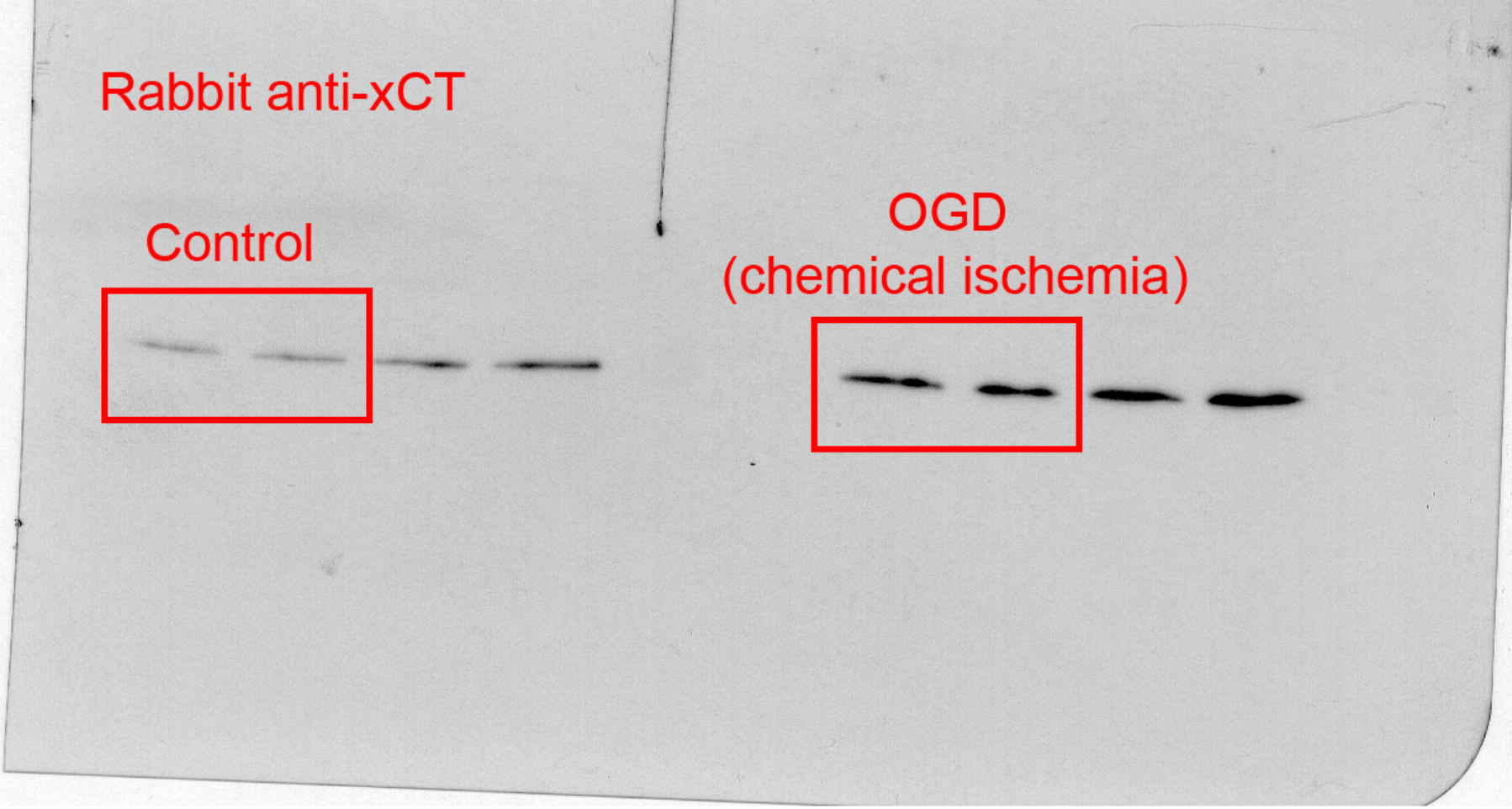

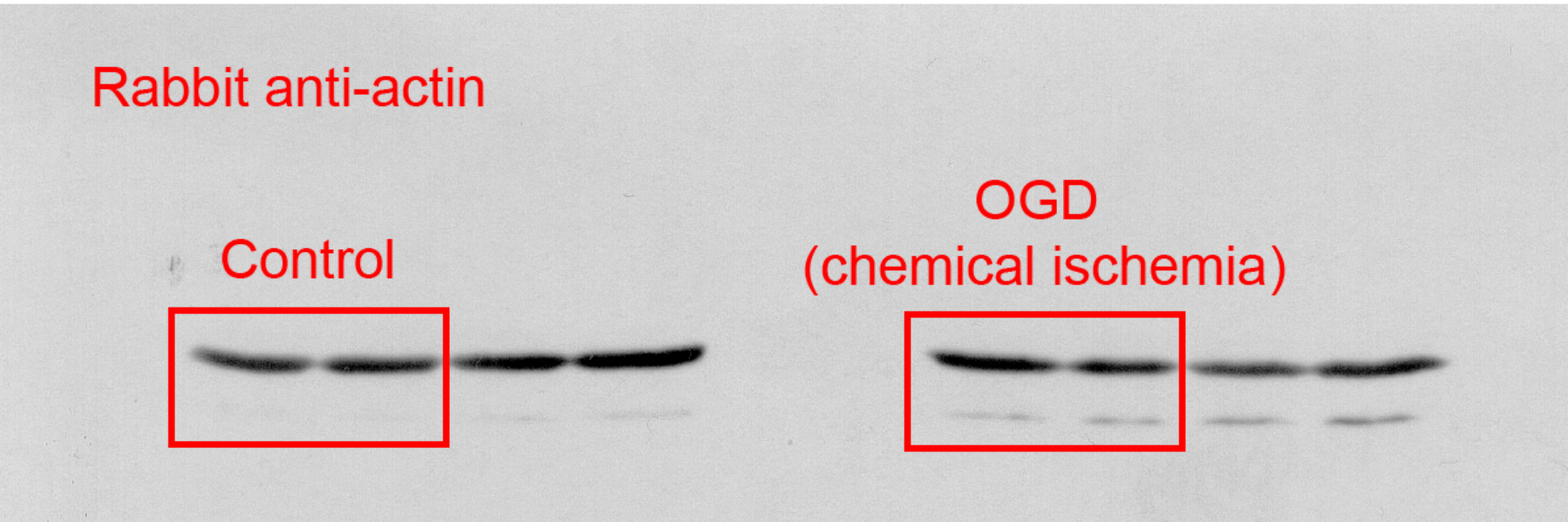

MW of xCT band (40 kDa) was determined by 2 different MW markers
(run in the middle of these 8 lanes, hence the blank space)
However, MW of the xCT band can be infered from the faint residual signal under the actin (45 kDa) band.
(the membrane was reprobed for actin after xCT)